Effect of Defects on the Electrical Properties of 4H-SiC Schottky Barrier Diodes

Takashi Katsuno, Yukihiko Watanabe and Tsuyoshi Ishikawa

Report received on Jan. 25, 2012

■**ABSTRACT**‖　The effect of defects on the electrical properties of 4H-SiC Schottky barrier diodes (SBDs) was investigated. Nanoscaled circular cone-shaped pits (nanopits) were observed at the leakage current sources of 4H-SiC SBD using atomic force microscopy (AFM). The leakage currents were generated due to the concentration of electric fields at the nanopits during measurement of the reverse bias characteristics. The positions of the nanopits correspond to the positions of threading dislocations (TDs), which were identified from molten potassium hydroxide (KOH) etching. The most important factor of leakage current generation was determined to be the surface morphologies of the TDs rather than their presence. Furthermore, there is no difference in the sensitivities on the leakage currents between threading screw dislocations (TSD) and threading edge dislocations (TED), because both nanopit shapes are almost the same. As a result, the leakage currents of 4H-SiC SBDs were proportional to the etch pit density (EPD) obtained from both TSDs and TEDs.

1. Introduction

Silicon carbide (SiC) is a suitable material for use in next-generation power devices, because it has superior thermal, mechanical, and electrical properties compared to silicon (Si).[1-3] The high breakdown field of SiC material enables high power densities to be realized in SiC devices. Consequently, SiC power devices are highly suitable for use in a variety of applications, such as power conversion in electric vehicles (both fully cell-powered and hybrid vehicles). SiC power devices require several-hundred-ampere diodes with low specific on-resistance. In addition, high reliability and high reproducibility of the electrical properties are required. The advantages of 4H-SiC Schottky barrier diodes (SBDs) are high switching speeds and low switching losses due to low surge currents during high frequency operation, and many groups have investigated 4H-SiC SBDs with high electrical performance.[4-7] However, dispersion of the electrical properties in 4H-SiC SBD diodes, ranging from low blocking voltage to high leakage current, is observed and is mainly caused by the influences of surface and crystalline defects.[8-12]

Micropipes and downfalls are generally the cause of low blocking voltage in the reverse bias characteristics of 4H-SiC SBDs.[8,9] Different sensitivities to other surface defects, such as triangular defects in 4H-SiC epilayers, have been reported by many groups,[13,14] but these defects mainly cause an increase of the leakage current in the reverse bias characteristics of 4H-SiC SBDs.

Furthermore, various sensitivities of the reverse characteristics to threading dislocations (TDs) have also been reported.[13-19] Some reports have noted the influence of TDs on the leakage current,[13-16] and contrasting reports have not noted such an influence by TDs.[18,19] We suggest that the surface morphologies at the leakage current sources of 4H-SiC diodes are changed, and this is a possible reason for the different sensitivities. Step bunching on SiC surfaces is known to cause an increase of the leakage current;[20,21] therefore, it is suspected that unusual surface morphology may be observed at the leakage current sources.

To confirm the change of surface morphology at leakage current sources, the leakage current sources of 4H-SiC SBDs were determined using emission microscopy, and their surface morphologies were investigated using atomic force microscopy (AFM). Molten KOH etching was then performed to assist identification of crystalline defects and to determine

the presence of TDs at the leakage current sources. The etch pit density (EPD) of 4H-SiC diodes on crystalline defects by molten KOH etching were investigated to clarify the relationship between the dispersed reverse characteristics of 4H-SiC SBDs and the crystalline defects.

2. Experimental Methods

A 4° off-axis n-type 4H-SiC repeated a-face (RAF) substrate with a 13 µm thick epitaxial layer doped with 5.0×10^{15} cm^{-3} of nitrogen was used to fabricate 4H-SiC SBDs. A field-limiting ring (FLR) was used as a termination structure, and the breakdown voltage was designed to be approximately 1400 V. The SiC surface was chemically cleaned by immersion in H_2SO_4/H_2O_2 solution for 10 min, and Al was implanted at a dose of 1×10^{19} cm^{-3} to complete the FLR structure. The FLR structure was then annealed at 1600 °C for 30 min to remove damage due to the creation of defects by Al implantation. Ti/Ni layers were deposited on the backside and annealed at 900 °C for 30 min to ensure the formation of an ohmic contact. A 100 nm thick, 400 µm diameter Mo layer was deposited on the surface as a Schottky electrode and an Al electrode (4000 nm thick) was deposited on the Mo electrode. The reverse bias characteristics of the 4H-SiC SBD were measured to evaluate the electrical properties. An emission microscope (Hamamatsu Photonics PHEMOS-1000) was used to determine the leakage current sources of the 4H-SiC SBD. A cooled CCD image sensor with a sensitivity range of 300 to 1100 nm was equipped in the emission microscope. The leakage current (emission current) of 4H-SiC SBD was observed through the partially-polished backside electrode using the CCD image sensor. A reverse voltage of 1200 V was applied between the surface and backside. Visual markings with points approximately 10 µm apart from the sources of the emission currents were applied using a focused ion beam (FIB) from the surface side to assist location of the leakage current sources. After removal of the surface electrodes by H_2SO_4/H_2O_2 solution for 10 min, the surface morphologies of the leakage current sources around the visual markings were measured by AFM (Veeco Nanoscope V); the observation areas for leakage current sources were 2 µm squares. After measuring the surface morphologies of the leakage current sources, the presence of crystalline defects (e.g., TSDs, TEDs, and basal plane dislocations (BPDs)) corresponding to the positions of

the leakage current sources was determined.

Crystalline defects were transformed into etch pits by molten KOH etching at 500 °C for 5 min, which were then observed using laser microscopy (Keyence VK-9710).

3. Results and Discussion

Typical reverse characteristics of 4H-SiC SBDs are shown in **Fig. 1**. The blocking voltage of the 4H-SiC SBD was kept over 1200 V and the leakage level was less than 10^{-3} A/cm^2 at 1200 V. It was evident that the reverse properties were dispersed. The leakage current seems to follow a thermionic field emission model.[22] In this device, the Schottky barrier height Φ_B is 1.1 eV calculated from the forward characteristic, and the electric field strength at 1200 V is 1.5 MV/cm.

Figure 2 shows an emission microscope image of the 4H-SiC SBD, of which the sample is the middle leakage current level shown in Fig. 1. Six emission current points with various intensities (determined by
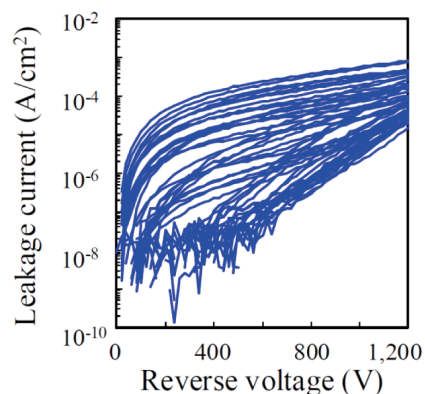
Fig. 1 Reverse bias characteristics of 4H-SiC SBDs measured at room temperature.
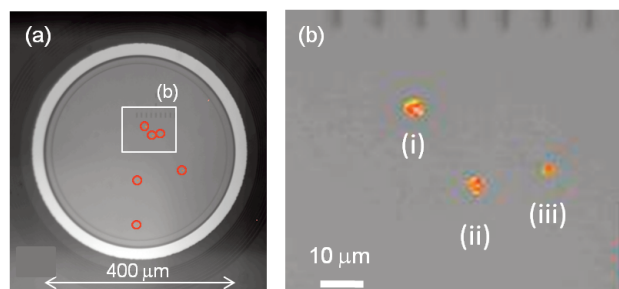
Fig. 2 Emission microscope images of 4H-SiC SBD at 1200 V. (a) View of the entire electrode. (b) Enlarged view of emission points (i), (ii) and (iii).

the contrast), as indicated by the circles in Fig. 2(a), were detected in the 400 μm diameter device. Strong intensity (contrast) indicates a high leakage current. Figure 2(b) shows an enlarged view of 3 emission current points, where the intensities of positions (i) and (ii) are almost the same, and the intensity of position (iii) is weaker than those of (i) and (ii). The visual markings produced by FIB are visible at the upper edge of Fig. 2(b).

AFM was used to investigate the surface morphologies at the leakage current sources. **Figures 3**(a) and (b) show the surface morphologies of the leakage current sources at positions (i) and (ii) shown in Fig. 2, respectively. The different color contrast indicates that the surface morphologies of leakage current sources (i) and (ii) are not flat. To confirm the shapes of the leakage current sources, line profiles measured between the arrows shown in Figs. 3(a) and (b) are presented in Figs. 3(c) and (d), respectively. Very small circular cone-shaped pits are evident at the leakage current sources. The pit at position (i) is 240 nm wide and 48 nm deep with a base angle of 136°, as shown in Fig. 3(c). The pit at position (ii) is 220 nm wide and 44 nm deep with a base angle of 136°, as shown in Fig. 3(d). In contrast, the pit at position (iii) is 230 nm wide and 20 nm deep with a base angle of 160°. These pits are nanosized and are therefore referred to as nanopits. It should be noted that these are not etch

pits caused by molten KOH etching. The shapes of the nanopits at positions (i) and (ii) are very similar. The positions of the leakage current sources correspond to the positions of the nanopits. The maximum field strength was applied at the interface of the SiC surface and Mo (Schottky metal) during the reverse bias measurement due to the presences of the pits, and the electric fields concentrate at the nanopits; therefore, leakage currents are generated at the nanopits.

Figure 4(a) shows simulation results of nanopits (d_{pit} = 50 nm, α_{pit} = 120°) on the SiC surface, where the pits cause an increase of the reverse leakage current in the
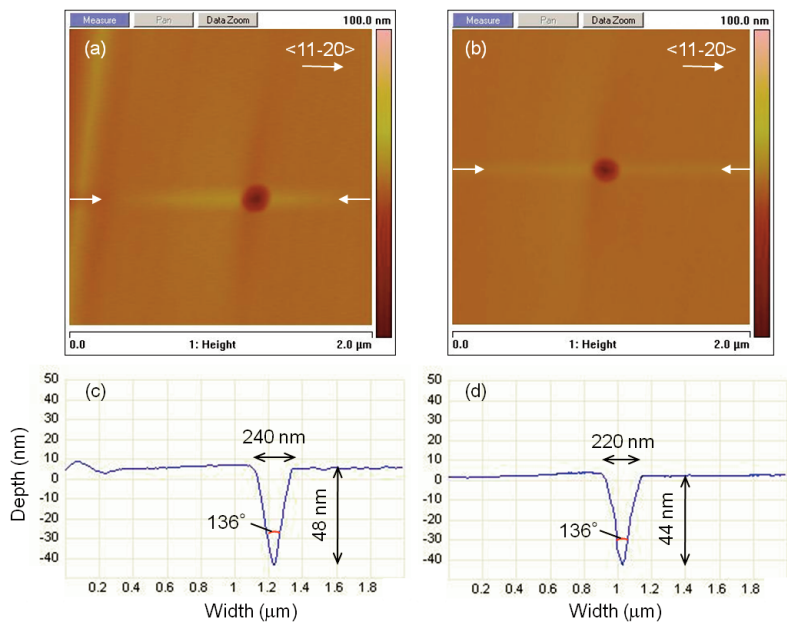
Fig. 3 AFM images of leakage current sources (i) and (ii). Surface morphology of (a) position (i), and (b) position (ii). Line profiles of (c) the nanopit in (a) and (d) the nanopit in (b).
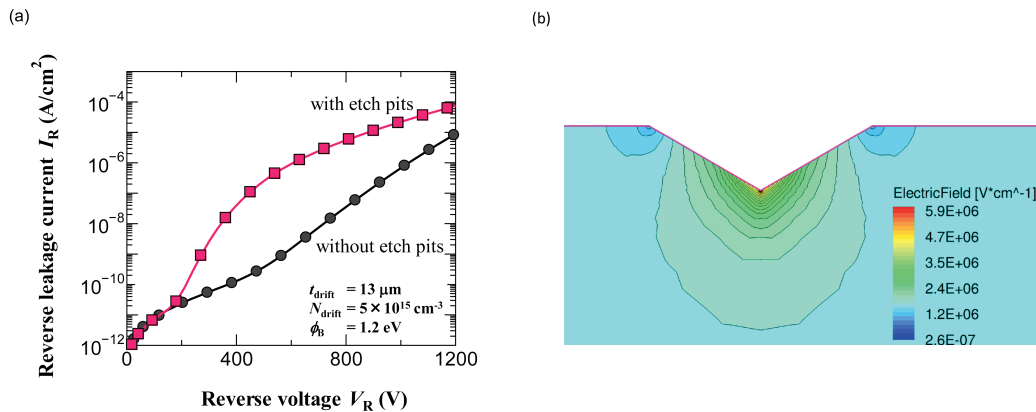
Fig. 4 (a) Comparison of reverse *I-V* curves with (α_{pit} = 120°, d_{pit} = 50 nm, n-EPD: 35400 cm^{-2}) and without etch pits (flat surface). (b) Contour plot of electric field at V_R = 1200 V around the etch pit.

reverse voltage.[23] This leakage current is due to electron tunneling current at the bottom of the nanopit. This tunneling current is caused by the electric field enhancement at the bottom of nanopit. The electric field at the metal-semiconductor interface (Schottky junction) near the bottom of pits is four times greater than that of a flat surface area with application of reverse voltage $V_R = 1200$ V, as shown in Fig. 4(b).

Figure 5 shows the simulation result for the impact of the nanopit shape (depth d_{pit}, and opening angle α_{pit}) on the leakage current.[23] Although the leakage current is sensitive to both d_{pit} and α_{pit}, no significant increase in the leakage current is observed in the depth range of less than 20 nm. There is a good relationship between the emission intensities and the nanopit depths at positions (i) and (ii); both the depths of the nanopits and the emission intensities are also the same. The intensity of position (iii) is weaker than that at
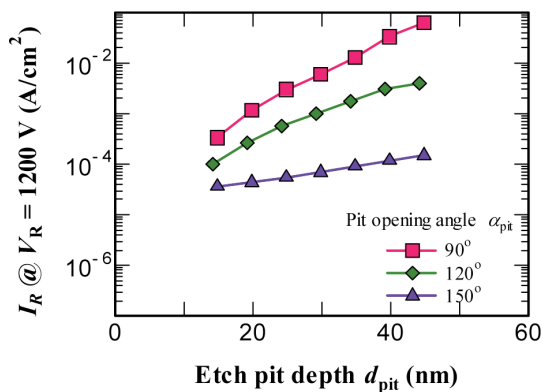
positions (i) and (ii) in Fig. 2(b) and the depth of the nanopit at position (iii) is only 20 nm. Accordingly, the leakage current at position (iii) is lower than that at positions (i) and (ii), due to the lower electric field than that at positions (i) and (ii).

To confirm the surface morphologies of the leakage current sources, different leakage current sources were also measured by AFM. Surprisingly, nanopits were present at all emission points (total: n=24) in some 4H-SiC SBDs. The distributions of the nanopit depth, width and base angle are summarized in **Figs. 6**(a)-(c), respectively.[24] TEDs (n=22/24) and TSDs (n=2/24) are represented by the hatched and gray fills, respectively. There is no difference in the nanopit shapes of the TSDs and TEDs. Thus, the sensitivities of TSD and TED to the leakage current are almost the same. As proposed, the presence of nanopits is an important factor in the increase of the leakage current.

The relationship between the positions of the nanopits and crystalline defects was confirmed by laser microscopy observation of the etch pits formed by molten KOH etching. Six etch pits denoted by circles are evident in **Fig. 7**(a), the positions of which correspond to the emission points shown in Fig. 2(a). Figure 7(b) shows an enlarged view of the 3 etch pits with the same field of view as that in Fig. 2(b). The positions of the nanopits (equal to the leakage current sources) also correspond to the positions of TDs. From the shapes of the etch pits, the crystalline defects at positions (i) and (iii) are identified as TEDs and that at position (ii) appears to be a TSD. TSDs are generally more sensitive than TEDs with respect to the leakage current;[12,13,15] however, this is not in agreement with the results, because the sensitivities of TSDs and TEDs to the leakage current are almost the same. Figure 4(b)

Fig. 5 Dependence of leakage current I_R (at $V_R = 1200$ V) on the opening angle α_{pit} and depth d_{pit} of etch pits. (n-EPD: 1.27×10^6 cm^{-2}).
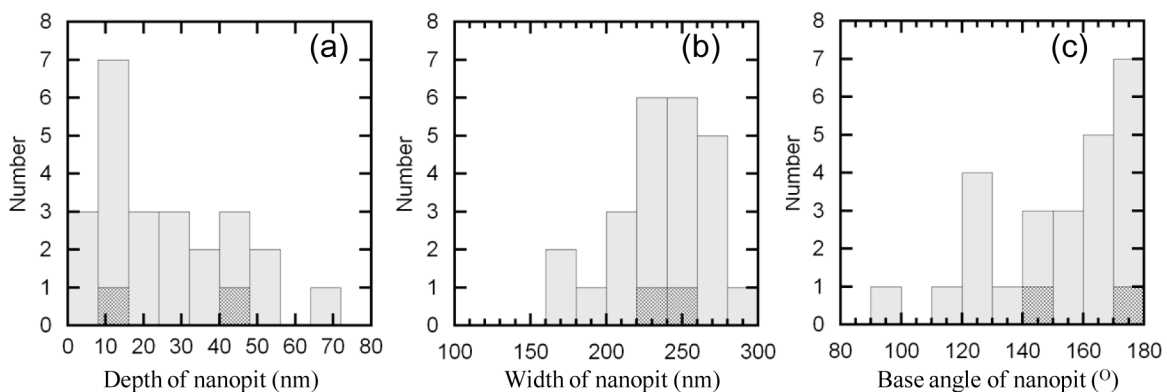
Fig. 6 Distribution of nanopit (a) depth, (b) width and (c) base angle in 4H-SiC SBDs.

shows that the TDs at positions (i) and (ii) are different, although the emission intensities are almost the same, as shown in Fig. 2(b). Therefore, the leakage current is not dependent on the type of crystalline defect (TSD or TED), but is dependent on the presence of nanopits and their respective depths. Therefore, the factor of leakage current generation is the surface morphology of the TD rather than the presence and type of TD.

The relationship between leakage current and EPD calculated from the medium and small etch pits formed from TSDs and TEDs, respectively, were investigated. BPDs, which produce shell pits by molten KOH etching, were not observed in the samples under analysis; thus, BPDs are not discussed in this paper. The numbers of etch pits (both TSDs and TEDs) in the area of interest were counted. **Figure 8** shows the relationship between the EPD and the leakage current at 1200 V. The leakage current increases at an almost constant rate with the EPD from 10^3 to 10^4 cm^{-2}. Based on this trend, the etch pits from TDs are considered to increase the leakage current by approximately 10^{-8} A/cm^2. Due to the content of nanopits in these samples, the leakage current increases with increasing EPD.

The creation of nanopits is influenced by the presence of TDs; however, it is unclear why the nanopits are created. TDs are crystalline defects, and the top of TDs at SiC surfaces can be easily damaged by thermal conditions due to the weak bonds at TDs. Therefore, it is possible that the nanopits are present in a bare epi-wafer or are produced during device processing. It has been reported that TDs do influence the leakage current,[13-16] yet other reports suggest that there is no influence of TDs on the leakage current.[18,19] We propose that both results are correct.
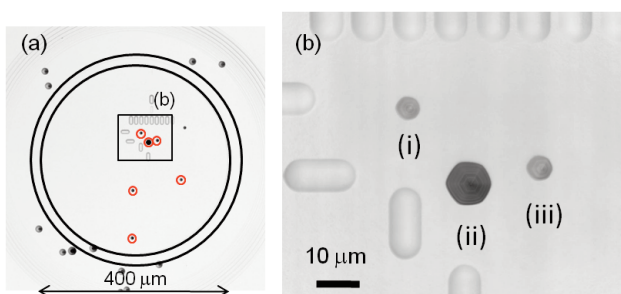
The 4H-SiC SBDs samples investigated by the former groups had nanopits (corresponding to the position of TDs), which generate the leakage current. In contrast, the samples of the latter groups did not have nanopits (or the surfaces were extremely flat), and therefore no leakage current was generated, and no dependence on TDs was evident.

In this study, Mo was used as a Schottky barrier metal for the 4H-SiC SBD. The leakage currents caused at the nanopits would be influenced by different Schottky barrier metals such as Ti, Ni, and Au. However, the nanopits of the 4H-SiC PN diodes would not influence the leakage currents, because the position of maximum electric field strength is the PN junction formed below the SiC surface and not the nanopits on the SiC surface. Therefore, the increase of leakage currents caused at nanopits would be dependent on the structures (SBD, junction barrier Schottky (JBS) and PN diodes).

4. Conclusions

In summary, the leakage current sources of 4H-SiC SBDs were analyzed using AFM. The leakage current sources have nanoscaled circular cone-shaped pits (nanopits). The electric field at the nanopits is concentrated during measurement of the reverse bias characteristics and leakage currents are generated. The positions of the nanopits correspond to the positions of TD etch pits, which were determined by molten KOH etching. The important factor in the generation of the leakage current is the surface morphology of the TD rather than the presence and type of TD. Therefore, the sensitivities of TSD and TED on the leakage

Fig. 7 Laser microscope image of 4H-SiC SBD after molten KOH etching. (a) View of the entire electrode. (b) Enlarged view of emission points (i), (ii) and (iii) in the same field of view as that shown in Fig. 2(b).
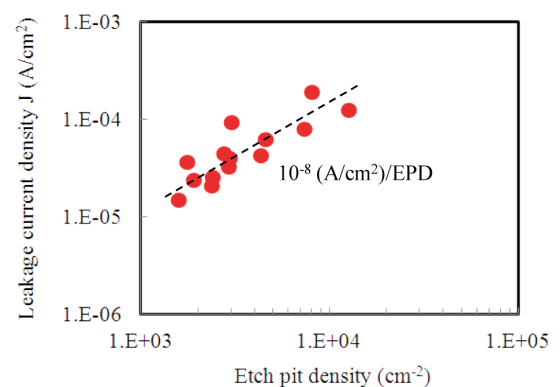
Fig. 8 Relation between EPD and the leakage current of 4H-SiC SBDs at 1200 V.

current are almost the same.

Acknowledgements

References

(1) Ruff, M., et al., "SiC Devices – Physics and Numerical-simulation", *IEEE Trans. Electron Devices,* Vol.41 (1994), pp.1040-1054.

(2) Kimoto, T., et al., "Performance Limiting Surface Defects in SiC Epitaxial p-n Junction Diodes", *IEEE Trans. Electron Devices*, Vol.46 (1999), pp.471-477.

(3) Casady, J. B. and Johnson R. W., "Status of Silicon Carbide (SiC) as a Wide-bandgap Semiconductor for High-temperature Applications: A Review", *Solid-State Electron.*, Vol.39 (1996), pp.1409-1422.

(4) Singh, R., et al., "SiC Power Schottky and PiN Diodes", *IEEE Trans. Electron Devices*, Vol.49 (2002), pp.665-672.

(5) Tumakha, S., et al., "Defect-driven Inhomogeneities in Ni/4H-SiC Schottky Barriers", *Appl. Phys. Lett.*, Vol.87 (2005), 242106.

(6) Ewing, D. J., et al., "Inhomogeneities in Ni/4H-SiC Schottky Barriers: Localized Fermi-level Pinning by Defect States", *J. Appl. Phys.*, Vol.101 (2007), 114514.

(7) Skromme, B. J., et al., "Electrical Characteristics of Schottky Barriers on 4H-SiC: The Effects of Barrier Height Nonuniformity", *J. Electro. Mater.*, Vol.29 (2000), pp.376-383.

(8) Neudeck, P. G., "Electrical Impact of SiC Structural Crystal Defects on High Electric Field Devices", *Mater. Sci. Forum*, Vol. 338-342 (2000), pp.1161-1166.

(9) Kamata, I., et al., "Electroluminescence Analysis of Al+ and B+ Implanted pn Diodes", *Mater. Sci. Forum*, Vol.389-393 (2002), pp.1137-1140.

(10) Fujiwara, H., et al., "Characterization of In-grown Stacking Faults in 4H-SiC (0001) Epitaxial Layers and Its Impacts on High-voltage Schottky Barrier Diodes", *Appl. Phys. Lett.*, Vol.87 (2005), 051942.

(11) Lee, K.-Y. and Capano, M. A., "The Correlation of Surface Defects and Reverse Breakdown of 4H-SiC Schottky Barrier Diodes", *J. Electron. Mater.,* Vol.36 (2007), pp.272-276.

(12) Grekov, A., et al., "Effect of Crystallographic Defects on the Reverse Performance of 4H-SiC JBS Diodes", *Microelectron. Reliab.*, Vol.48 (2008), pp.1664-1668.

(13) Wahab, Q., et al., "Influence of Epitaxial Growth and Substrate-induced Defects on the Breakdown of 4H-SiC Schottky Diodes", *Appl. Phys. Lett.*, Vol.76 (2000), 2725.

(14) Berechman, R. A., et al.,"Electrical and Structural Investigation of Triangular Defects in 4H-SiC Junction Barrier Schottky Devices", *J. Appl. Phys.*, Vol.105 (2009), 074513.

(15) Izumi, S., et al., "Analysis for Structural Defects in the 4H-SiC Epilayers and Their Influence on Electrical Properties", *Mater. Sci. Forum*, Vol.457-460 (2004), pp.1085-1088.

(16) Katsuno, T., et al., "Effects of Surface and Crystalline Defects on Reverse Characteristics of 4H-SiC Junction Barrier Schottky Diodes", *Jpn. J. Appl. Phys.*, Vol.50 (2011), 04DP04.

(17) Katsuno, T., et al., "Analysis of Surface Morphology at Leakage Current Sources of 4H-SiC Schottky Barrier Diodes", *Appl. Phys. Lett.*, Vol.98 (2011), 222111.

(18) Morisette, D. T. and Cooper, J. A., "Impact of Material Defects on SiC Schottky Barrier Diodes", *Mater. Sci. Forum*, Vol.389-393 (2002), pp.1133-1136.

(19) Saitoh, H., et al., "Origin of Leakage Current in SiC Schottky Barrier Diodes at High Temperature", *Mater. Sci. Forum,* Vol.457-460 (2004), pp.997-1000.

(20) Syvajarvi, M., et al., "Step-bunching in SiC Epitaxy: Anisotropy and Influence of Growth Temperature", *J. Cryst. Growth*, Vol.236 (2002), pp.297-304.

(21) Guy, O. J., et al., "Improved Schottky Contacts to Annealed 4H-SiC Using a Protective Carbon Cap: Investigated Using Current Voltage Measurements and Atomic Force Microscopy", *Diamond Relat. Mater.*, Vol.15 (2006), pp.1472-1477.

(22) Hatakeyama, T., et al., "Optimum Design of a SiC Schottky Barrier Diode Considering Reverse Leakage Current due to a Tunneling Process", *Mater. Sci. Forum*, Vol.433-436 (2002), pp.831-834.

(23) Ishikawa, T., et al., "Critical Density of Nanoscale Pits for Suppressing Variability in Leakage Current of a SiC Schottky Barrier Diode", *Mater. Sci. Forum*, (2012), in print.

(24) Katsuno, T., et al., "Surface Morphology of Leakage Current Source of 4H-SiC Schottky Barrier Diode by Atomic Force Microscopy", *Mater. Sci. Forum,* (2012), in print.

Takashi Katsuno
  Research Field:
    - Development of Compound
      Semiconductor Power Devices
  Academic Degree: Ph. D
  Academic Society:
    - The Japan Society of Applied Physics

Yukihiko Watanabe
  Research Field:
    - Development of SiC Power Devices
  Academic Degree: Dr. Eng.
  Academic Societies:
    - The Japan Society of Applied Physics
    - IEEE Electron Device Society

Tsuyoshi Ishikawa
  Research Field:
    - Development of Semiconductor Power
      Devices
  Academic Degree: Dr. Eng.
  Academic Societies:
    - The Japan Society of Applied Physics
    - The Japanese Society of Microscopy